



## Deposition Tantalum Pentoxide Coating on 2101 Lean Duplex Stainless Steel by Reactive Sputtering for Biomedical Applications

Nesreen Dakhel Fahad<sup>1</sup>, Jassim M. Salman Al-Murshdy<sup>2</sup>, Ali Sabea Hammood<sup>1</sup>

<sup>1</sup> Department of Materials Engineering, Faculty of Engineering, University of Kufa, Iraq

<sup>2</sup> Babylon University, College of Materials Engineering, Iraq.

Received 20 June 2021; Received in revised form 5 Aug. 2021; Accepted 15 Aug. 2021; Available online 1 Nov. 2021

### Abstract

The most recent advancement in implant development is to meet materials that accelerate bone formation at the interface of bone implant and improve Osseo integration. Lean Duplex Stainless Steel as an implantation material needs several enhancements to the surface's properties chemically and physically. The application of surface modifications over the implant is an important method for improving the surface properties of LDX. Reactive Sputtering has some benefits for surface modification, including changing surface topography, increasing hardness and surface roughness, improving surface antibacterial activity and adhesion strength. Coating LDX 2101 DSS with Ta<sub>2</sub>O<sub>5</sub> at times (2,4,6,8, and 10) hrs was used by a modified reactive sputtering technique. Analysis of surface characterization for samples before and then after the sputtering process was performed by micro hardness test, "x-ray diffraction", XRD analysis, "scanning electron microscope", SEM, and "field emission scanning electron microscope" (FE.SEM), "energy dispersive spectroscopy" (EDS), "Atomic force microscope" (AFM), Antibacterial study and Adhesion strength were done on the samples surfaces and compared to uncoated one. The current results indicate that the formation of Ta<sub>2</sub>O<sub>5</sub> layers on the surface of the alloy was achieved, which would improve the surface characteristics, hardness, inhibited bacterial activity and adhesion strength of LDX 2101 DSS for orthopedic applications.

**Copyright © 2021 International Energy and Environment Foundation - All rights reserved.**

**Keywords:** Lean Duplex 2101 stainless steel; Tantalum nitride; Reactive sputtering; Biomedical applications.

### 1. Introduction

"Duplex stainless steels" have microstructures comprising a biphasic of austenite " $\gamma$ " and ferrite " $\alpha$ " [1, 2], both presented in almost equal amounts in the material. New types of DSS with noticeable amount of nitrogen (close to 0.2%), no Mo and very low Ni (less than 2%) were advanced in all continents. The recent DSS is more lean than standard DSS in alloying, when in view of mechanical properties and total costs of alloying element [3]. The high Cr and N content of LDX, combined with an adding of Mo, offer better resistance to uniform and localized corrosion and exhibits both larger strength and better resistance of chloride stress corrosion cracking than traditional stainless steels of 300 series [4]. LDX 2101, UNS S32101, "lean duplex stainless steel" has a balanced microstructure by low Ni content and alloyed with N

and Mn [5]. Lean duplex stainless steels (LDX) are essential for many applications such as: [6] outlet duct reinforcements and External absorber, air Pollution Control, Pressure vessels, Biofuels, Palm oil, Pulp and Paper, Food and Beverage Process Equipment, Infrastructure and wine storage tanks, Chemical processing, Power generation and also new areas of applications such as architecture, green energy, stainless rebar's, water systems and desalination. Lean duplex stainless steel grades have little Ni and little Mo, better mechanical properties, but lowest pitting resistance. Cases of LDX are 2002 (UNS S32002), 2101 (UNS S32101) and 2304 (UNS S32304). In 2016 (Jian Cheng) [7], in order to improve the corrosion and wear resistance of biomedical implants, a Ta<sub>2</sub>N nano ceramic coating was synthesized on a Ti-6Al-4V alloy by the double glow discharge plasma process. The Ta<sub>2</sub>N coating showed higher corrosion resistance than both commercially pure Ta and uncoated Ti-6Al-4V in this solution. In 2018 (Ay Ching Hee) [8], Tantalum films were deposited on negatively biased Ti6Al4V substrates using filtered cathodic vacuum arc deposition to enhance the corrosion resistance of the Ti6Al4V alloy showed a significant improvement in corrosion resistance, which is attributed to the stable oxide layer. In 2020 (Hassan Jawad Farhan) [9], aim of study to evaluate the effect of TaN coating by modified plasma sputtering technique of commercially pure titanium disk on wettability, surface roughness, surface chemical composition in comparison to non-coated surface to find materials which accelerate bone formation at bone implant interface and improve Osseo integration.

Nowadays the main target is the development of lean duplex having much less allowing elements than the standard duplex grade. The target is the replacement of 316 and even 304 grades. Industeel produces 2202 and 2304 lean duplex grades, which offer excellent cost effective alternatives to 304L and 316L in a number of applications) [10].

## 2. Experimental Procedures

### 2.1 Material and Methods

For rod form, LDX 2101 DSS alloy (provided by Sweden Outokumpu factory) was cut with a wire cut machine (knuth smart DEM manufactured in Germany) to (15x5) mm a diameter and a thickness as shown in Figure 1. Table 1 shows the chemical structure of the "LDX 2101" DSS alloy.



Figure 1. Sample prepared experimentally.

Table 1. Chemical composition of LDX 2101 DSS alloy.

| LDX 2101 Stainless Steel Alloy | EN     | ASTM   | C    | Cr   | Ni  | Mo  | N    | Others   | Fe  |
|--------------------------------|--------|--------|------|------|-----|-----|------|----------|-----|
|                                | 1.4162 | S32101 | 0.03 | 21.5 | 1.5 | 0.3 | 0.22 | 5 Mn, Cu | Bal |

### 2.2 Surface Modification with sputtering Ta<sub>2</sub>O<sub>5</sub>

By using reactive sputtering system, the sputtering technique was performed. The sputtering procedure started with placing the cleaned and polished samples on the center of base of anode electrode. evacuating process of chamber to high vacuum ( $\approx 1 \times 10^{-5}$  mbar) using system with high vacuum consist of turbo and rotary molecular vacuum pumps to confirm the whole removing of the heavy gases like hydrocarbons. Power supply (negatively charged voltage 3.5 kV). For sputtering process, the voltage was gradually applied using variance until the required energy achieved (applied voltage and current), the pressure was  $5 \times 10^{-2}$  mbar and this pressure was achieved by feeding the bombardment and reactive gases. The appropriate voltage and amber were adjusted precisely by regulator until intended sputtering glow (purple color, which standardized for each gas) is achieved. So the cathode placed in upper part and anode electrode placed in lower part of chamber. A Target (cathode) and anode disk of stainless steel. With a 7 cm gap between them, the cathode faces the anode, providing an electric field for the gas to be released. The bottom of the stainless steel disk cathode electrode is covered with tantalum pentoxide sheet which stared as target.

The clean and polished samples were placed on the anode in the center of base which regarded as substrate. The anode was joined to the D.C. source of power, while the cathode was connected to the grounded chamber. The process was carried out at various sputtering times (2, 4, 6, 8 and 10 hrs). After the sputtering process completed, the samples were kept until ambient temperature in the vacuum chamber was reached.

### 2.3 Characterization of Samples

"Optical microscopy" (OM) was used to detect the phases of ferrite and austenite before sputtering. Surface morphology of sputtering samples observed by using SEM, "LEITS-type", "FESEM", ("ZEISS-type microscopes") at different times, as well as estimating of thickness, affected depth of coating layer of reactive sputtering process. A micro hardness tester (TH715, Time High Technology Ltd, China) was used to determine hardness of coating layer. Nikon's, ("EclipseME600, Digital Camera DXM 1200F microscopy"), made in China, was used to OM examination, with a magnification of "X500-X1000", and identification of phases formed during reactive sputtering performed by "X-ray diffraction" (XRD) ("The Shimadzu Lab X XRD- 6000, Japan"), a copper target ( $K\alpha$  radiation = 0.15418 nm) with a nickel filter was used to perform the test. The diffractometer's scanning speed was adjusted to 5 degrees per minute, and the diffraction angle range was adjusted at 20–80 degrees. Chemical structures and relative concentrations for non-coated and coated LDX 2101 DSS with Ta<sub>2</sub>O<sub>5</sub> discs were assessed via energy dispersive spectroscopy (EDS) while (Ra) "surface roughness" of the Ta<sub>2</sub>O<sub>5</sub> coated samples was measured using an AFM (SPMAA3000, Angstrom Advanced Inc., USA) on a chosen surface area.

### 2.4 Adhesion Test

The adhesion was measured with Rockwell-C adhesion test; it uses tester of a standard Rockwell hardness fit by Rockwell (Type-C) diamond cone by an applied load (150 kg). Rockwell hardness test was carried out on untreated LDX 2101 DSS and sputtered samples with Ta<sub>2</sub>O<sub>5</sub>.

### 2.5 Antibacterial Test

Biomaterials surfaces is susceptible to microbial colonization and bacterial attack; thus it was necessary to study the antibacterial activity of plasma sputtered samples then the application of this alloy in the orthopaedic applications. The antibacterial activity and antibacterial kinetics of Escherichia coli, a gram positive bacteria, were studied using the inhibition zone method. The bacteria were then spread around a petri dish containing "Mueller Hinton agar," and "0.5 mL" of suspension was added to the dish, which was then hugged at 37 °C for 24 hrs.

## 3. Results and Discussion

### 3.1 Characterization of Main Materials (LDX 2101 DSS)

LDX 2101 duplex stainless steel before surface modifications has microstructure biphasic, with darker "ferritic" and brighter "austenitic" phase grains in nearly area portion of 50.6 % ferrite ( $\alpha$ ) and 49.4 % austenite ( $\gamma$ ) without secondary phases (Figure 2), that calculated by using Image J-1.46r program, which is in agreement with reference [11].

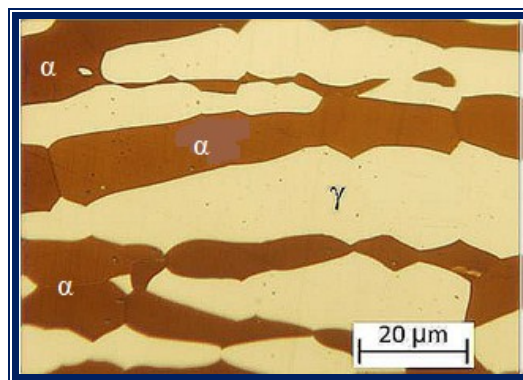


Figure 2. Main microstructure of LDX 2101 DSS, with "ferrite" (dark) and "austenite" (light) phases.

### 3.2 Characterization of Sputtering Samples

#### 3.2.1 Micro-Hardness Study

A ferritic structure (interstitial solid solution, mostly N; substitutional solid solution, mostly Cr, Mo, Ni; grains refinement, with mutual action between the phases) promotes mechanical resistance in the LDX 2101 DSS alloy, whereas an austenitic structure offers ductility and fracture toughness [12]. Figure 3. shows schematic diagram of micro hardness values of samples coated with Ta<sub>2</sub>O<sub>5</sub> at different times (2,4,6,8 and 10) hrs. It may be notice from this figure that when sputtering time increases, leads to increase the micro hardness of sputtered samples with Ta<sub>2</sub>O<sub>5</sub>. When compared to the as-sputtered sample, the hardness value of Ta<sub>2</sub>O<sub>5</sub> thin film was remarkably raised up to 1.7-fold. The increase in values of hardness may be because the crystallization phase of Ta<sub>2</sub>O<sub>5</sub> [13].

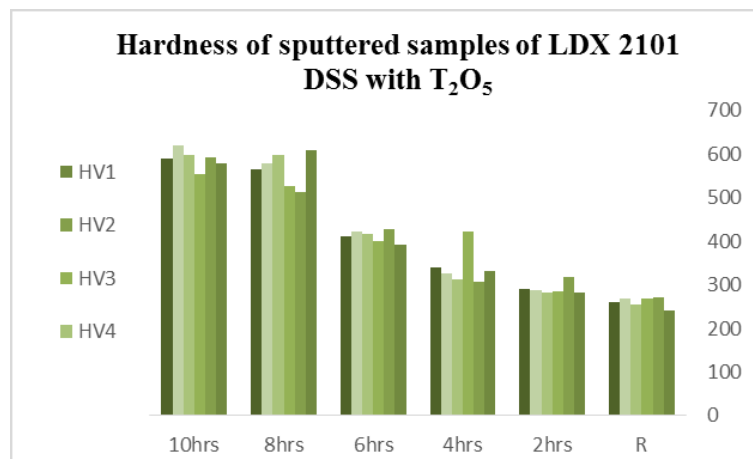


Figure 3. Illustrates schematic diagram of micro Hardness values of sputtered LDX 2101 DSS samples with Ta<sub>2</sub>O<sub>5</sub>.

#### 3.2.2 Field Emission-Scanning Electron Microscopy

The morphology of as sputtered and sputtered samples and topography were observed by SEM in Figure 4 (a,b,c,d,e), it displays the SEM micrographs of Tantalum pentoxide layer coatings at different times. The SEM surface micrograph displays a smoother surface, which is typical of compact coatings with amorphous morphologies, indicating that the addition of (O<sub>2</sub>) increases the coatings' densification. It can be observed that the microstructure was densely packed and contain a homogeneous particles distribution within them and lead to the formation of homogeneous coatings as they appeared in this Figure 4 (a and b) shows a cracked conglomerate structure with nonhomogeneous particles distribution within them at (2 and 4) hrs. On the other hand, after 10 hrs as shown in Figure 4 (e), it can be observed that there are micro cracks, coarse particles with non-uniform distribution and high percent of porosity (some discovered areas). Using of high time during sputtering led to a large increase in the porosity of deposition and the trend for formation of crack. Also, particles which form coarse will deposit, then cause an increase in the roughness and thickness of coating and that would promote the cracking to be more dominant for the thick layer as seen in Figure 4 (e). Therefore, it is clear that the coated sample at 8 hrs is the most appropriate one.

This little porous structure plays an important character in the biological performance of a bioactive layers, as it improves the bonding ability in addition to biocompatibility of the biometallic implants and permits bone growth and the easily fixation of implant. Figure 4 (a,b,c,d,e) illustrates the cross-sectional topography of sputtering samples with Ta<sub>2</sub>O<sub>5</sub> at (2,4,6,8 and 10) hrs. It's apparent that the sputtered layer has a regular thin film structure with more compact, homogeneity, and perfect adhesion between the coating and the substrate, with thicknesses of (454.19, 784.92, 867.54, 1.03, and 2.07) nm. Can be concluded that with the increase of sputtering time, thickness of coating layer increases significantly [14]. Interfaces can be seen clearly between sputtering layer and substrate. As well as Figure 4 shows mapping of elements that present in sputtering Ta<sub>2</sub>O<sub>5</sub> samples which are O, Cr, Fe, Ni and Ta that match with EDS analysis (Figure 5). The image of scanning electron microscopy of the sputtered coatings with Ta<sub>2</sub>O<sub>5</sub> ceramic shown a quite smooth and regular surface without cracks [15].

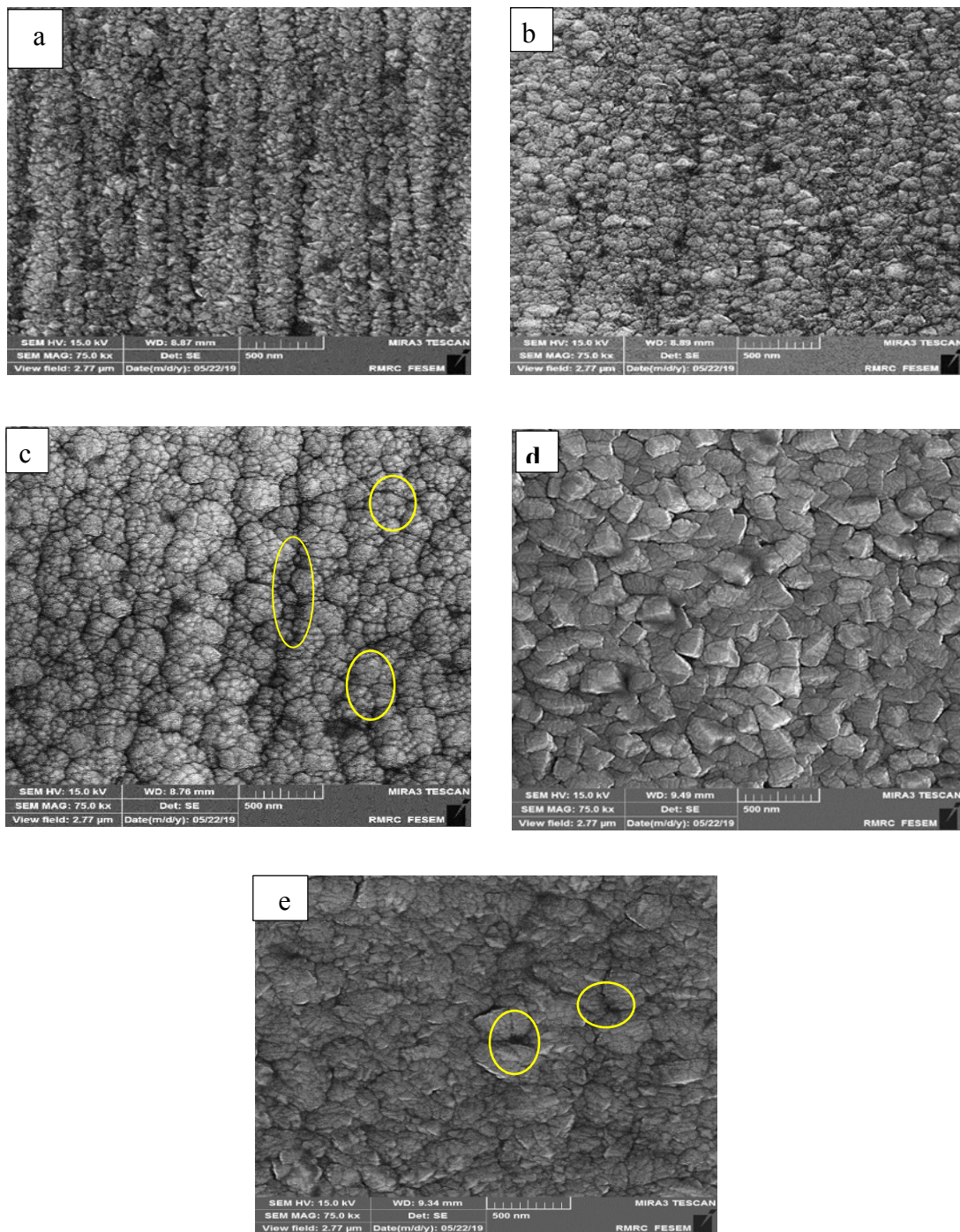


Figure 4. SEM micrographs of Tantalum Oxide coating on LDX 2101 DSS alloy at: (R) uncoated (a) 2 (b) 4 (c) 6 (d) 8 (e) 10 hrs.

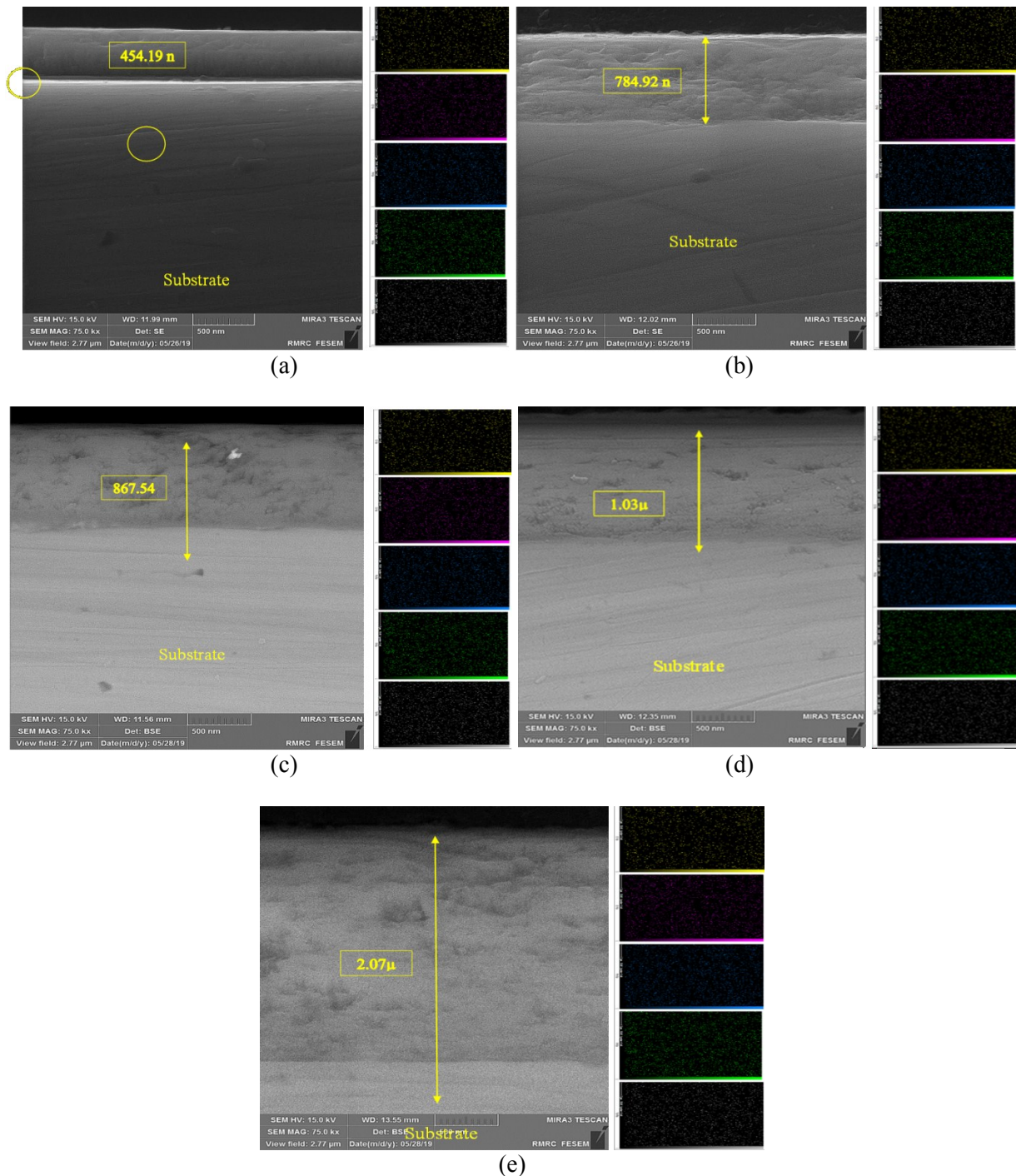


Figure 5. Illustrates cross-sectional "SEM" micrographs and "EDS" mapping of Tantalum Oxide coating on LDX 2101 samples at: (a) 2 (b) 4 (c) 6 (d) 8 (e) 10 hrs.

### 3.2.3 Energy Dispersive Spectroscopy (EDS)

Figure 6 show EDS results, it can be observed that Fe, Cr, O, Ta and Ni are the main elements which existing in the sputtered layer for coated samples at conditions (2,4,6,8 and 10) hrs sputtering time. The presence of these elements confirm the successful formation of a Tantalum Oxide layer on the LDX 2101 duplex stainless steel alloy. Moreover, there is no other peaks different from  $Ta_2O_5$  and this assure the coating purity. Table 2 illustrate these elements percent for each sample.

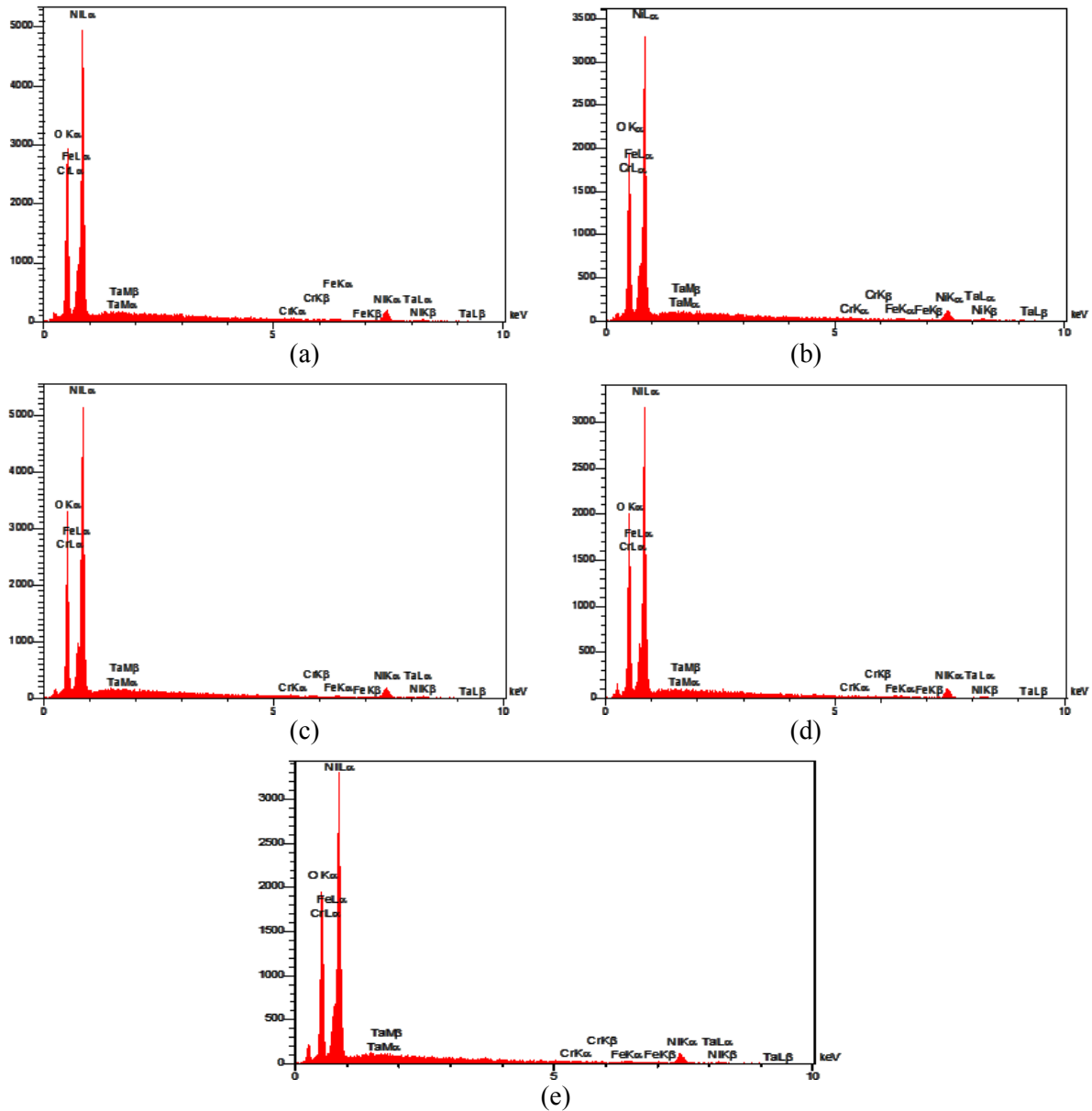


Figure 6. EDS for sputtering coated samples with  $Ta_2O_5$  at condition: (a) 2, (b) 4, (c) 6, (d) 8, (e) 10 hrs.

Table 2. Elements Percent of  $Ta_2O_5$  coating on LDX 2101 DSS.

| No. | Condition | Fe%  | Cr%  | O%    | Ni%  | Ta%   |
|-----|-----------|------|------|-------|------|-------|
| A   | 2 hrs     | 2.13 | 0.46 | 31.17 | 0.31 | 65.94 |
| B   | 4 hrs     | 2.10 | 0.59 | 30.86 | 0.29 | 66.15 |
| C   | 6 hrs     | 2.44 | 0.43 | 30.36 | 0.32 | 66.46 |
| D   | 8 hrs     | 0.67 | 0.33 | 34.31 | 0.50 | 64.19 |
| E   | 10 hrs    | 1.34 | 0.42 | 33.65 | 0.64 | 63.95 |

### 3.2.4 X-Ray Diffraction (XRD) Analysis

The results of XRD analysis, (Figure 7), revealing crystalline  $\alpha$  and  $\gamma$  phases in the reference (untreated) LDX sample, after sputtering  $Ta_2O_5$  film crystallization possess a typical amorphous hump between  $2\theta$  angle of  $20^\circ - 40^\circ$ .  $Ta_2O_5$  (Tantalum Pentoxide) in all the surfaces [12]. In this study,  $Ta_2O_5$  coatings are synthesized by using a reactive magnetron sputtering system. The deposited  $Ta_2O_5$  exhibited amorphous structure. The as-deposited sputtered  $Ta_2O_5$  coatings observed an amorphous structure, i.e., no peaks were detected [15]. There were no diffraction peaks identified in the Ta-O coatings. However, a detailed

examination of the diffraction pattern shown a broad diffraction peak in the  $2\theta$  range of  $20\text{--}40^\circ$ , indicating that the structure is nanocrystalline. Also, the broad peak of the pattern matches with the position of some peaks for oxide phases such as orthorhombic  $\text{Ta}_2\text{O}_5$  (ICDD card no 00–025-0922), tetragonal  $\text{TaO}_2$  (ICDD card no 00–019-1297) and, indicating that just one or a mixture of these phases can be found [16].

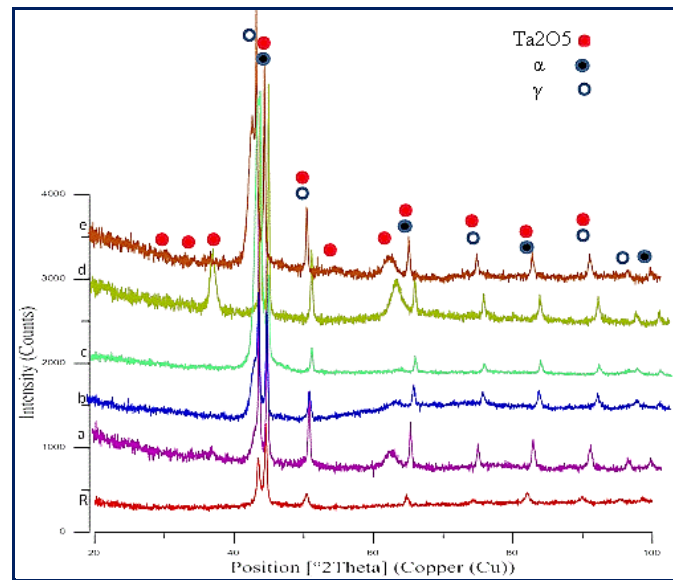


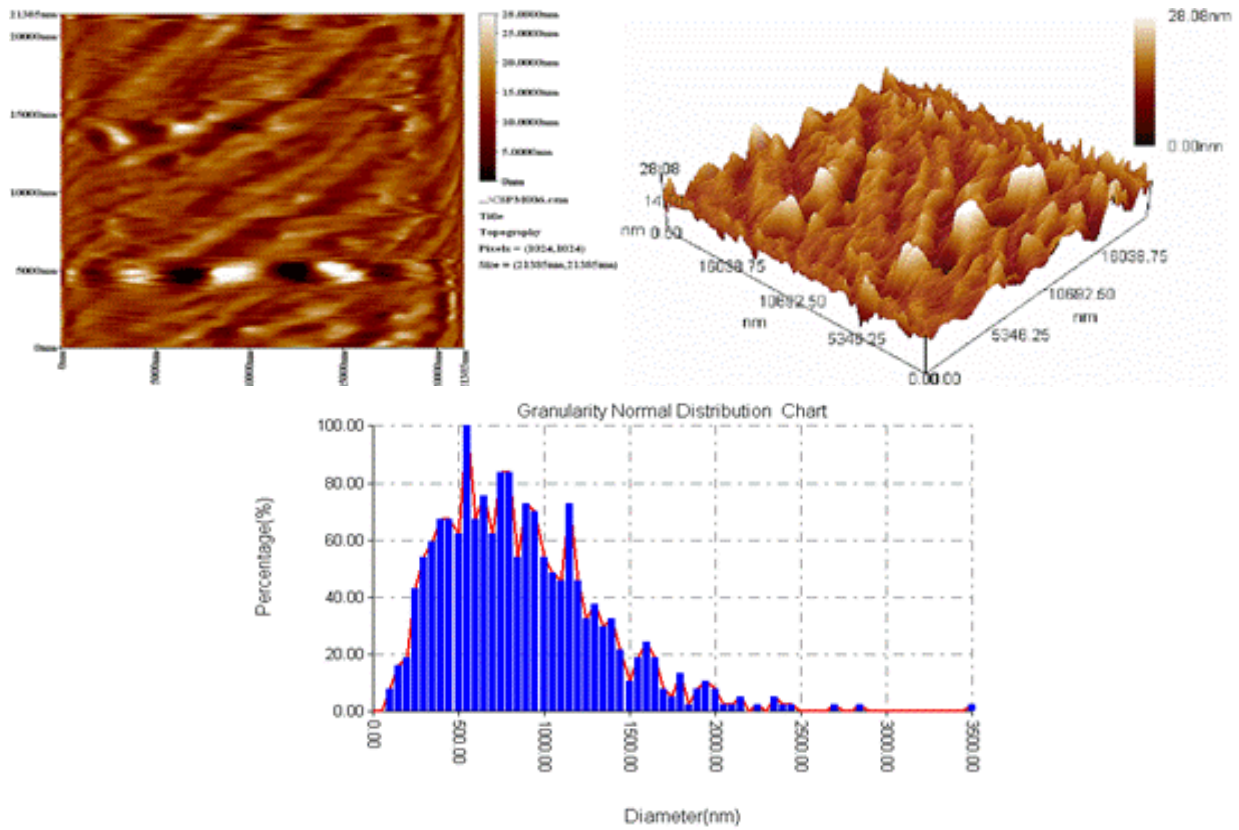
Figure 7. XRD patterns of coated LDX 2101 samples with Tantalum Oxide at condition: (R) un coated (a) 2 (b) 4 (c) 6 (d) 8 (e) 10 hrs.

### 3.2.5 Atomic Force Microscopy analysis

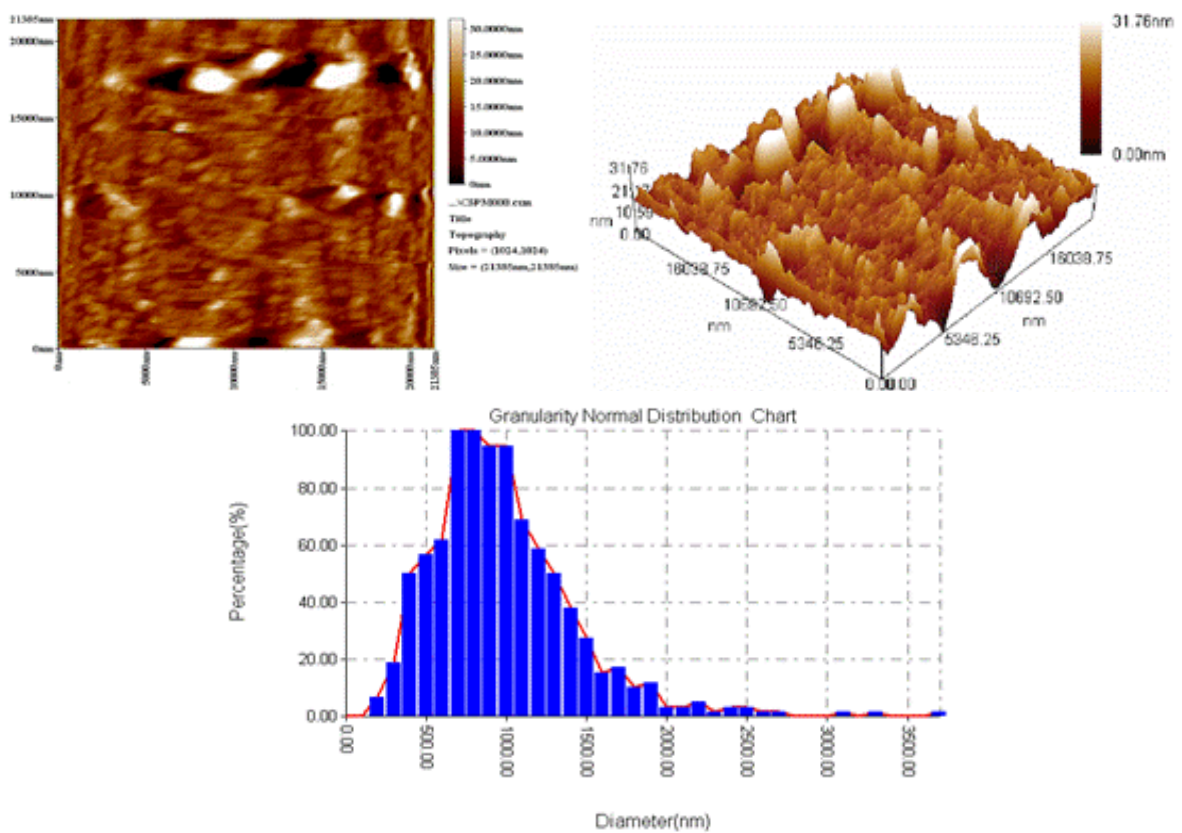
The AFM analysis is performed for the substrate LDX 2101 DSS and sputtering samples with  $\text{Ta}_2\text{O}_5$  at (2,4,6,9 and 10) hrs. The topography of the sputtered samples and different particles distribution in  $\text{Ta}_2\text{O}_5$  coating layer with 3D performance image is shown in Figure 8. The surface roughness of sputtered coated samples was (2.65, 2.71, 3.22, 3.6 and 6.11) nm, which indicate that when time of sputtering increased, thickness of sputtering coating layer increased [9]. This Figure also show different particles distributions for the mentioned samples. It appears that the granularity accumulations for the coating layers with average diameters of (846.92, 934.69, 1032.25, 1109.00 and 1196.36) nm in these conditions that the irregular distribution of particles on the  $\text{Ta}_2\text{O}_5$  surface increases with increasing sputtering time [12, 15].

### 3.2.6 Antibacterial Study

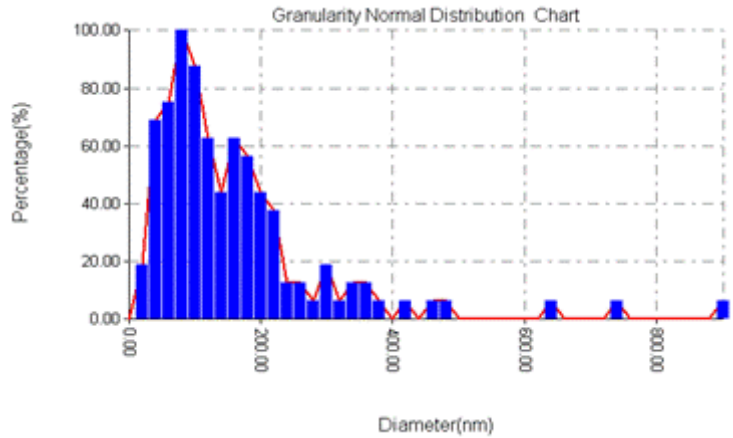
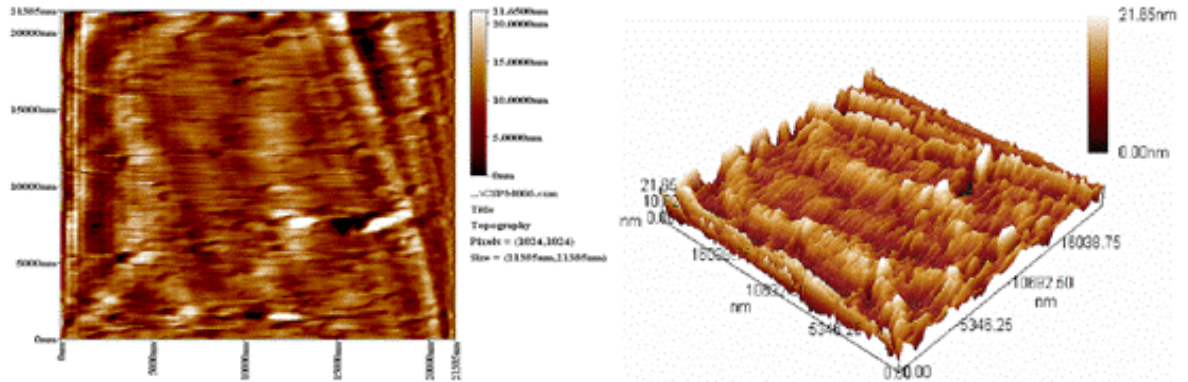
Figure 9 shows that the deposited  $\text{Ta}_2\text{O}_5$  coating has a stronger antibacterial effect than the uncoated alloys. The amorphous and crystalline  $\text{Ta}_2\text{O}_5$  exhibits good antibacterial activity against *E. Coli*, depending on the coating structures (amorphous and crystalline phases), and has promise in medical applications.  $\text{Ta}_2\text{O}_5$  coatings possess excellent cell viability and are able to be used as a coating layer for implant applications for improving biocompatibility. The changes of structure in tantalum oxides surfaces during modification result in the formation of a bioactive tantalite layer on the surface of metallic tantalum in SBF, which contains alkali ions and can accelerate the spontaneous nucleation of bone-like apatite.



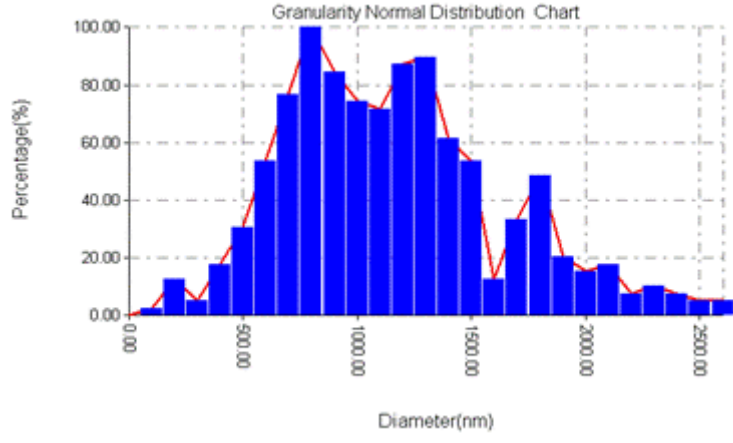
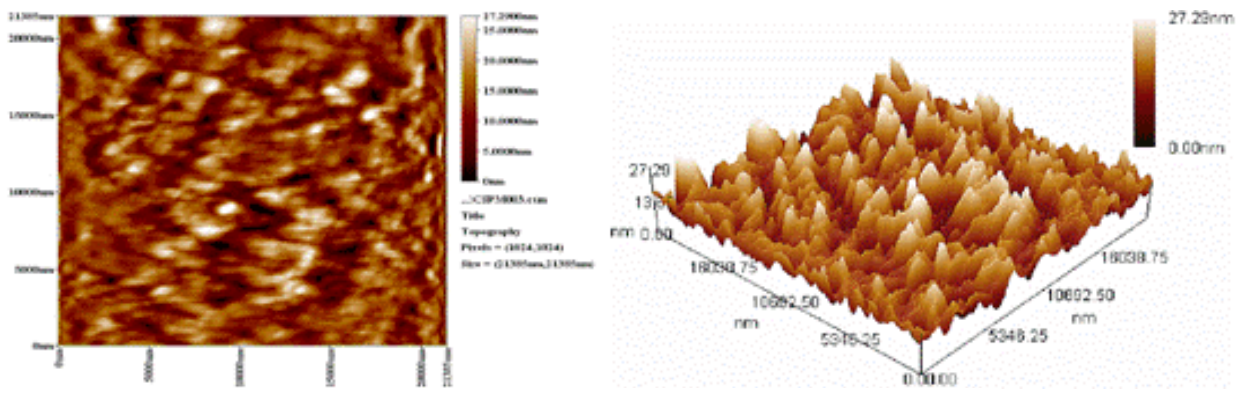
(a)



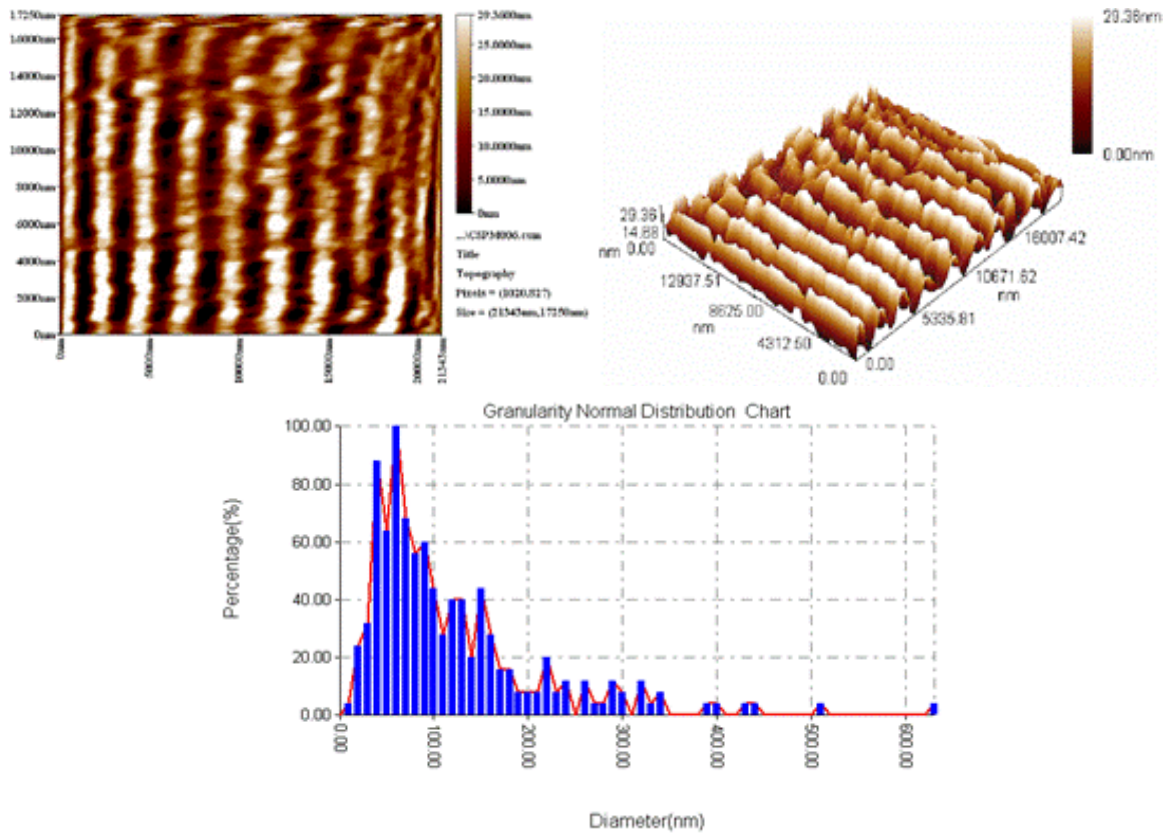
(b)



(c)



(d)



(e)

Figure 8. The topography of the Tantalum Oxide coated samples with 3D performance images and Granularity accumulation chart for particles at condition: (a) 2 (b) 4 (c) 6 (d) 8 (e) 10 hrs.

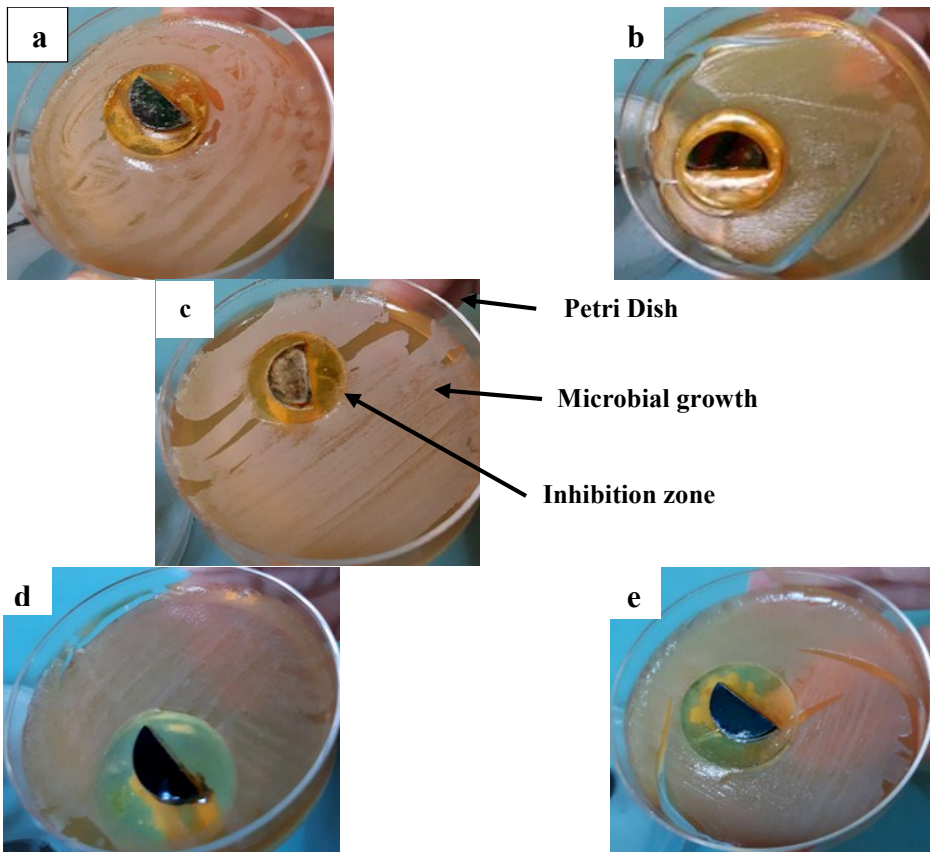


Figure 9. Optical photographs of antibacterial activity of E.coli performed for sputtering samples with Ta<sub>2</sub>O<sub>5</sub> at condition:(a) 2 (b) 4 (c) 6 (d) 8 (e) 10 hrs.

### 3.2.7 Adhesion Test

Figure 10 shows the Optical microscope (OM) images of Rockwell C indentation on the sputtered samples with  $Ta_2O_5$ . Shallow and short cracks are observed around the indentation point in the sputtering samples with  $Ta_2O_5$  at different times (2, 4, 6, 8 and 10) hrs. Furthermore, no delamination is observed around the Rockwell C indentation effect. The only cracking on any of these layers is minimal and located within the indentation. All samples coatings deposited by sputtering in this study have a HF rating of 1 that denotes all tantalum films exhibit good adhesion regardless of thickness. All coatings and layers revealed high adhesion. Moreover, the sputtering layer indicated minimal cracking demonstrating good adhesion to the substrate [12].

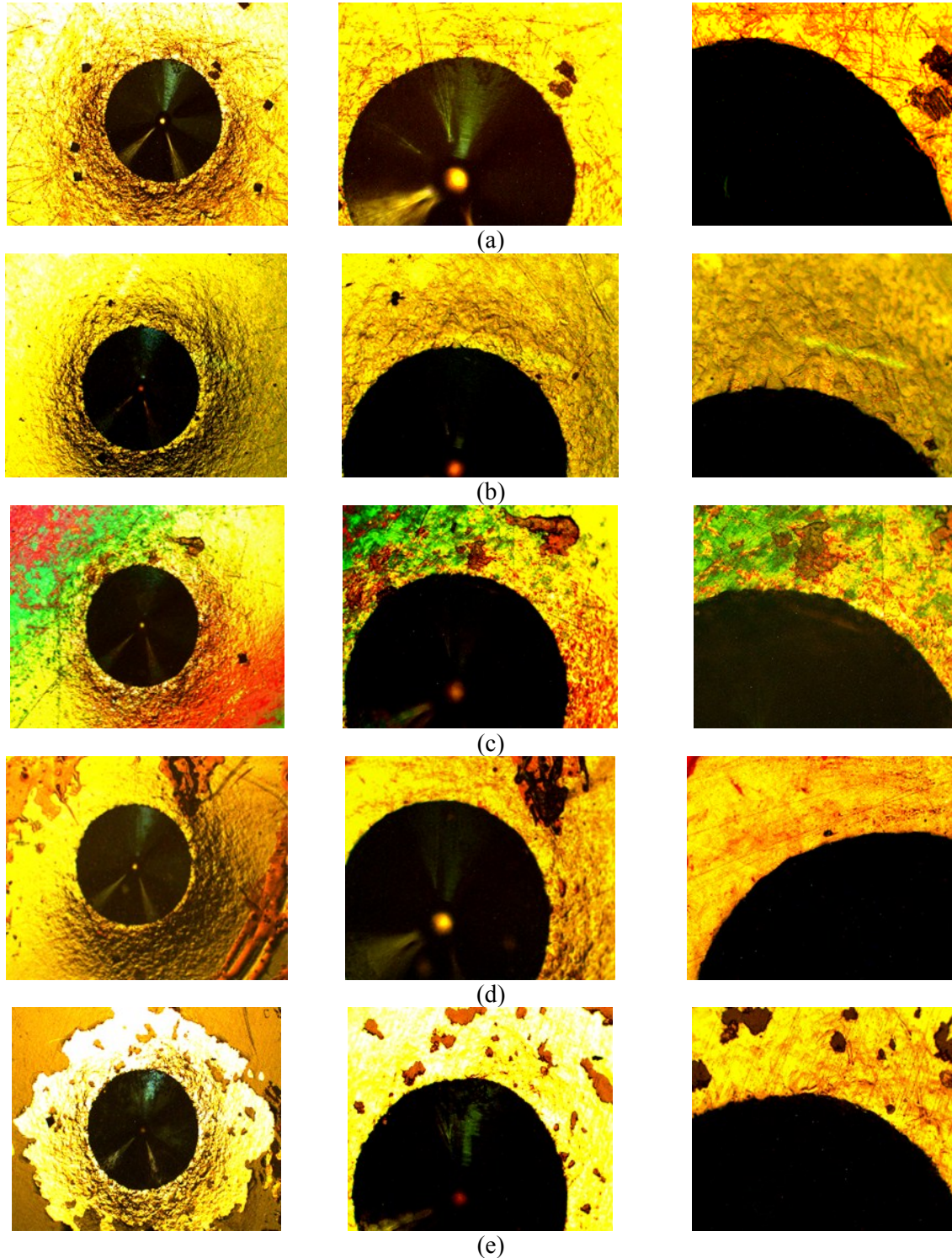


Figure 10. Optical photographs of Rockwell type - C effect an indentation for plasma sputtered samples at condition: (R) un treatment (a) 2 (b) 4 (c) 6 (d) 8 (e) 10 hrs.

#### 4. Conclusions

Conclusions that can be take out from the experimental results:

1. Reactive Sputtering of LDX 2101 DSS with Ta<sub>2</sub>O<sub>5</sub> results in a strengthening of the surface layer increasing in hardness, then decreasing based on the sputtering times.
2. FE-SEM and EDS micrographs demonstrate that the sputtered Ta<sub>2</sub>O<sub>5</sub> layer thickness formed on the surface of LDX 2101 increases as sputtering times increase.
3. Sputtering layer with Ta<sub>2</sub>O<sub>5</sub> has anti-bacterial activity vs. E.coli bacteria.
4. Coated Tantalum pentoxide has good adhesion between coating and substrate, so it can be used in biomedical applications.
5. Sputtering time at 8 hr was the optimal time condition for LDX 2101 lean duplex stainless steels for Orthopedic biomedical implants, according to the results of Ta<sub>2</sub>O<sub>5</sub> coated samples at times (2,4,6,8,10) hrs.

#### References

- [1] F. W. Abdulsada and A. S. Hammood, "Characterization of corrosion and antibacterial resistance of hydroxyapatite/silver nano particles powder on 2507 duplex stainless steel," *Mater. Today Proc.*, vol. 42, pp. 2301–2307, 2021.
- [2] A. S. Hammood, M. S. Naser, and Z. S. Radeef, "Electrophoretic Deposition of Nanocomposite Hydroxyapatite/Titania Coating on 2205 Duplex Stainless Steel Substrate," *Jom*, vol. 73, no. 2, pp. 524–533, 2021.
- [3] J. Charles, "Duplex families and applications : A review Part 2 : From 1991 to nowadays," no. September, pp. 67–70, 2015.
- [4] M. Gorog, "Duplex Stainless Steels," *Duplex Stainl. Steels*, no. November, pp. 1–437, 2014.
- [5] A. S. Hammood, "Biom mineralization of 2304 duplex stainless steel with surface modification by electrophoretic deposition," *J. Appl. Biomater. Funct. Mater.*, vol. 18, 2020.
- [6] A. M. L. Aalco, "Stainless Steel Stainless Steel," Carbon N. Y., 2018.
- [7] J. Cheng, J. Xu, L. L. Liu, and S. Jiang, "Electrochemical corrosion behavior of Ta<sub>2</sub>n nanoceramic coating in simulated body fluid," *Materials (Basel)*, vol. 9, no. 9, pp. 1–21, 2016.
- [8] A. C. Hee, H. Cao, Y. Zhao, S. S. Jamali, A. Bendavid, and P. J. Martin, "Cytocompatible tantalum films on Ti6Al4V substrate by filtered cathodic vacuum arc deposition," *Bioelectrochemistry*, vol. 122, pp. 32–39, 2018.
- [9] H. J. Farhan, R. K. Jassim, and L. Thair, "Deposition of ta<sub>2</sub>o<sub>5</sub> film on commercial pure titanium disk by modified reactive plasma sputtering technique," *Medico-Legal Updat.*, vol. 20, no. 1, pp. 1036–1041, 2020.
- [10] TMR Stainless, *Practical Guidelines for the Fabrication of Duplex Stainless Steels*. 2014.
- [11] W. Dou, "Surface Modification of Lean Duplex Stainless Steels by Low Temperature Plasma Nitriding," 2014.
- [12] B. Rahmati et al., "Development of tantalum oxide (Ta-O) thin film coating on biomedical Ti-6Al-4V alloy to enhance mechanical properties and biocompatibility," *Ceram. Int.*, vol. 42, no. 1, pp. 466–480, 2016.
- [13] R. Alias, R. Mahmoodian, K. Genasan, K. M. Vellasamy, M. Hamdi Abd Shukor, and T. Kamarul, "Mechanical, antibacterial, and biocompatibility mechanism of PVD grown silver–tantalum-oxide-based nanostructured thin film on stainless steel 316L for surgical applications," *Mater. Sci. Eng. C*, vol. 107, p. 110304, 2020.
- [14] M. Li, H. Cui, H. Wang, Z. Wang, and Y. Liu, "Performance Differences of Ta<sub>2</sub>O<sub>5</sub> Films under Different Magnetron Sputtering Conditions," vol. 126, no. *Icmmet*, pp. 920–923, 2017.
- [15] A. Zykova et al., "Surface modification of tantalum pentoxide coatings deposited by magnetron sputtering and correlation with cell adhesion and proliferation in in vitro tests," *J. Phys. Conf. Ser.*, vol. 700, no. 1, 2016.

- [16] H. Moreira, A. Costa-Barbosa, S. M. Marques, P. Sampaio, and S. Carvalho, "Evaluation of cell activation promoted by tantalum and tantalum oxide coatings deposited by reactive DC magnetron sputtering," *Surf. Coatings Technol.*, vol. 330, no. September, pp. 260–269, 2017.